Proceedings of the Korean Nuclear Society Spring Meeting
Gyeongju, Korea, 2004

Signal Processing Scheme and the Evaluation for the Five-Sensor Probe Method

Dong Jin Euh, Byong Jo Yun, Won Man Park, Young Jung Youn, Chul Hwa Song

Korea Atomic Energy Research Institute
P.O.Box 105, Yuseong, Daejeon, 305-600, KOREA

Ki Bong Baek

Chungbuk National Univ.
48 Gaesin-dong, Cheongju, Chungbuk, 361-763, KOREA

Abstract

Interfacial area concentration is one of the important parameters in the two-phase flow models. Five-sensor probe method is an useful measurement technique to measure the interfacial area cocentration. It is essentially based on the four-sensor probe method but improves it by adapting one more sensor. The passing types of the interfaces through the sensors are categorized into four and independent methods are applied to the interfaces belonging to each category. To verify the applicability of the five-sensor probe method, benchmarking tests are performed for the rectangular visual channel by using the photographic method. The bubble velocity, void fraction, and Sauter mean diameter measured by the probe are also benchmarked. In this study, the design of the five-sensor conductivity probe, the signal processing procedure of the probe signal and the data analysis method by photography are also described.

1. Introduction

In the formulation of two-fluid model, appropriate constitutive relations for the interfacial transfer terms are needed to close the phasic balance equations, and their accuracy significantly affects the results of the calculation. In general, the interfacial transfer terms are proportional to the interfacial area concentration (IAC), which is defined as the interface area per unit of fluid volume. Therefore, the IAC is one of the most important parameters in the two-fluid model and it is important to develop an accurate measuring method for the IAC. The probe method is a useful measurement technique for the two-phase flow parameters such as void fraction and bubble velocity. The measuring principle of the multi-sensor probe in obtaining a local time-averaged IAC is based on the mathematical formula given by Ishii (1975). Currently two types of probe methods have been used, which are the double- and the four-sensor method. Double-sensor probe method is based on some statistical assumptions of the two-phase flow characteristics. This method is practical and useful in the dispersed flow regime, but in the other regimes where the particle shape is irregular, its applicability is rather restricted.[2][3][4] The four-sensor probe method can predict the IAC without any assumptions of the bubble shape.[2][5][6][7] The local IAC can be obtained by measuring the three dimensional components of the velocity vector at the measuring points and the directional cosines of the sensors. However, due to the finite size of the probe, it may happen that one or more of the rear sensors cannot detect the interface. Four-sensor method includes the method for the interfaces that pass all of the sensors and that for the missing interfaces. In this study, the former is called the four-point method. The missing interface has a very steep shape and a large interfacial area concentration at the measuring point. The contribution of the IAC from such interfaces may be so substantial that it must be appropriately considered. The four-sensor probe method can predict the IAC of such interfaces with a special mathematical formula, but it still has limitations due to a lack of information on the interfaces.

Euh et al.(2001) proposed a five-sensor sensor method to improve the previous probe methods.[8] The five-sensor probe method proposed in their study is essentially based on the four-sensor probe method but is improved by adapting one more sensor. This method has an advantage that a more systematic approach for the missing bubbles can be made when compared with the classical four-sensor probe method. To verify the applicability of the five-sensor probe method, numerical tests were performed with the consideration of the bubble lateral movement.[9] In their study, an improved method considering the bubble lateral motion effects were proposed. The effects of the bubble size and the intensity of the bubble lateral motion on the measurement of the interfacial area concentration were also investigated. The bubble parameters related to the bubble fluctuation and interface geometry were determined by the Monte Carlo approach.

To verify the applicability of the five-sensor probe method, benchmarking tests are performed for the rectangular visual channel by a comparison with the photographic method. The channel has a 10X10mm rectangular cross-section and is 1 m long. The interfacial area concentration, void fraction, Sauter mean diameter and bubble velocity are measured by using the photographic method and compared with the probe data. In this study, the processing procedures of the raw signals from the probe are also described.

2. Five-Sensor Probe Method

A five-sensor conductivity probe consists of a sensing part, sensor supporter, probe body, connector, and enamel wires, and so on, as shown in figure 1. The sensor is made of stainless steel coated by gold to increase the electrical conductivity and finally coated by Teflon to insulate it electrically except for the sensor tip. The thickness of the bare needle is 0.18mm and the final coated sensor thickness is 0.25mm. Figure 2 includes the detailed features of the individual sensor of the five-sensor conductivity probe. The configuration of the five sensors and their tips are shown by figure 2(b). The lateral length between the symmetrical rear sensor tips is 1.0mm and the vertical distance between the central front and rear sensor tips is

2.0mm. The central rear sensor is 0.25mm away from the centerline.

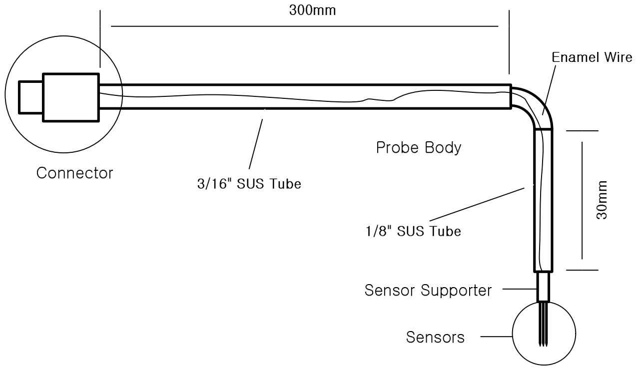

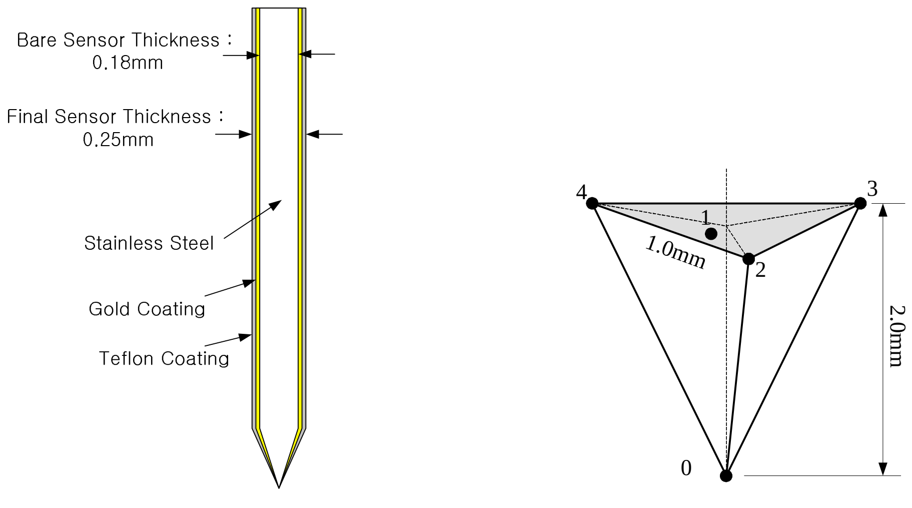

(a) (b)

Figure 2. Individual Sensor and Configuration of the Sensor Tips in the five-sensor probe

The configuration of the sensor tips and bubble interface that is projected onto a plane is shown in figure 3. The five-sensor method classifies the types of the interfaces passing through the sensors into four categories, and applies different mathematical formulations to each category. Category II and III interfaces are important missing interfaces that have a steep shape and a large interfacial area concentration at the measuring point. For category IV bubbles, the double sensor method is applied. Since very small bubbles can be regarded as a spherical shape and the double sensor method can be used, the small bubbles are also included in category IV although they follow the passing types of other categories. The five-sensor probe method adopts a different methodology according to each category and the details were presented in Euh et al. (2004)

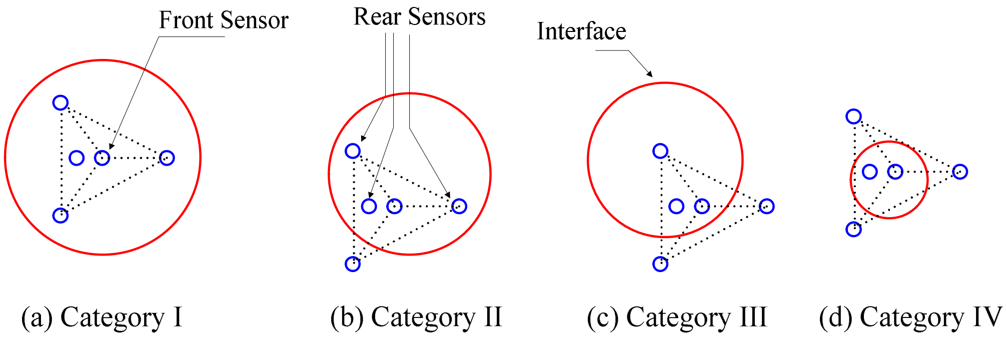

Figure 3. Categorization of the Bubble Passing Type through the sensors

3. Signal Processing Scheme

The external AC current is activated for the probe and the conductivity information of the two-phase mixture at the sensor tips is conveyed to the signals and then to the signal conditioner. A signal conditioner rectifies the AC currents and eliminates the high frequency components due to the noise by the low pass filter. The signals are then delivered to the terminal boards. Finally, the analog signals are converted to the digital signals with an A/D converter included in the IBM PC. At first, the digitalized raw signals should be converted to the rectangular forms. This process means an explicit definition of the phase. The following step is to find the same bubble signal in the two sensor signals. After finishing the above procedures, we can obtain various physical parameters such as the void fraction, velocity, interfacial area concentration, bubble frequency, bubble diameter, and so on. We used the overall processing environment of the HP-VEE. We set a 20 kHz sampling speed and used simultaneous sampling. The key process is performed by an external user function that is built by Visual C++.

Converting a raw signal to a rectangular form is an important process in obtaining the void fraction and bubble velocity. The process is done by 3-level steps for the digitalized raw signals. The first process is to find the average liquid level in the raw signals. The total counts are grouped to certain numbers for processing. Slope criterion, $\varepsilon 1$, and cutoff criterion of the raw signals are used to find the average liquid level. The cutoff criterion uses the value of the average liquid level of the previous counts group added by a factor. The procedures are repeated until the end of the counts.

The second process in converting the signals to the rectangular form is the main conversion part. The process includes various conditions to distinguish the phase. The conditions are summarized as follows.

a) If a signal level is above the liquid level and the right two consecutive signal slopes at an instant are above a certain criterion, $\varepsilon 2$, and positive, respectively, the signal means a gas phase. This condition is to find the bubble initiation point.
b) If a signal level is above the liquid level plus 20% of an average bubble height and the right two consecutive signal slopes are all positive, the signal means a gas phase.
c) If the previous count was for a gas phase and the right signal slopes at four consecutive

counts are all above a certain criterion, ε3, the signal means a gas phase. This condition is to find the bubble ending point. Here, a slightly negative slope criterion is used. The negative slope criterion is needed to prevent from finding the wrong bubble end point due to a minor bubble level fluctuation.

d) If a signal level is below the liquid level plus 20% of an average bubble height and the right three consecutive signal slopes are all less than a criterion, ε4, the signal means a liquid phase. This condition is to prevent any misleading conclusions due to a low-level signal fluctuation.

The final processing in converting the signals to a rectangular form is filtering. If the bubble width is very short, the bubble signal is neglected since it may be due to other noise sources. Figure 4 shows a typical signal conversion from the raw signals to a rectangular form following the above processing scheme.

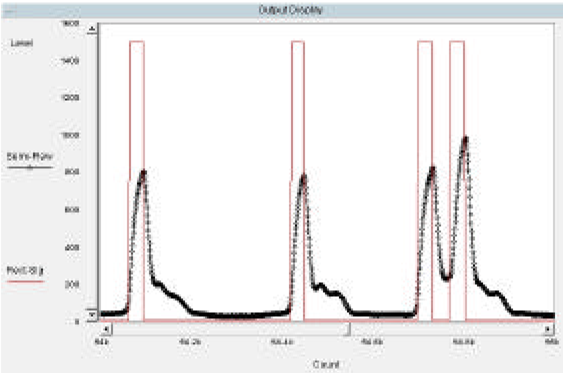

Figure 4. Converting Raw Signals to a Rectangular Form

The next processing after making the signals into the rectangular form is to find the same bubble signals in the front and rear sensor signals. We used the cross-correlation method with signals from front and each of the rear sensors. After the process, the bubble passing type defined by the five-sensor probe method is selected. For example, if you look at the signals in figure 5, the first peak occurs at all of the five sensor signals. Therefore, the bubbles are category I bubbles that contact with all of the sensors. However, the second peak does not appear at the rear sensor number 2. So, the second bubble is a category II one that bypasses one of the three peripheral rear sensors. The black line is a signal from the central front sensor and is prior to the other rear sensor signals as shown in the figure. If we measure the delay time, four velocities at the front sensor tip in the direction of each rear sensor can be obtained.

If the previous processes are completed, we can obtain various physical quantities such as the void fraction, bubble velocity, IAC, bubble diameter, and the chord length.

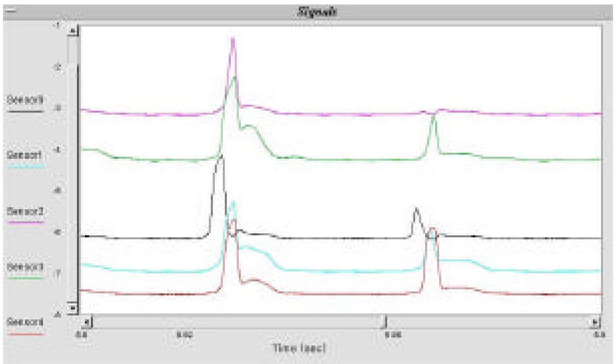

Figure 5. Overlapped Raw Signals

4. Uncertainty Analysis

The regression equations for the uncertainty analysis are summarized as follows.

a) Velocity

$$\mathrm{v_b} = \frac{d_{tip,v}}{t_{delay}} \tag{1}$$

b) Void Fraction

$$a = \frac{\sum t_b}{\Omega} \tag{2}$$

c) IAC

$$a_i \propto f(N_b, \mathrm{v}_i, t_b, d_{tip,v}, l_d) \tag{3}$$

d) Sauter mean diameter

$$D_{sm} = \frac{6a}{a_i} \tag{4}$$

In the above formulations, $d_{tip,v}$ and l_d are vertical and lateral length scale between sensor tips, respectively. The τ_b and Ω are the bubble residence time on the sensor tip and total problem time, respectively. The v_i, a_i, α, D_{sm}, and N_b are interface velocity, interfacial area concentration, void fraction, Sauter mean diameter and bubble frequency, respectively.

Since the IAC derivation from the five-sensor method is very complicated, we used the functional dependency to analyze the IAC uncertainty. The uncertainty analysis are then undertaken by the following:

$$\left(\frac{s(\mathrm{v}_b)}{\mathrm{v}_b}\right)^2 = \left(\frac{s(d_{tip,v})}{d_{tip,v}}\right)^2 + \left(\frac{s(t_{delay})}{t_{delay}}\right)^2 \tag{5}$$

$$\left(\frac{s(a)}{a}\right)^2 = \left(\frac{s(t_b)}{t_b}\right)^2 + \left(\frac{s(N_b)}{N_b}\right)^2 \tag{6}$$

$$\left(\frac{s(a_i)}{a_i}\right)^2=\left(\frac{s(N_b)}{N_b}\right)^2+\left(\frac{s(\mathrm{v}_i)}{\mathrm{v}_i}\right)^2+\left(\frac{s(t_b)}{t_b}\right)^2+\left(\frac{s(d_{tip,v})}{d_{tip,v}}\right)^2+\left(\frac{s(d_{tip,l})}{d_{tip,l}}\right)^2 \quad (7)$$

$$\left(\frac{s(D_{sm})}{D_{sm}}\right)^2=\left(\frac{s(a)}{a}\right)^2+\left(\frac{s(a_i)}{a_i}\right)^2 \quad (8)$$

The results of the uncertainty analysis for a 95% confidence are plotted in the benchmarking results together as shown in the later section (see figure 9).

5. Bubble Parameter Analysis Using Photographic Method

The data from the five-sensor conductivity probe is benchmarked by the photographic method. The signals from the probe are acquired for 2 minutes under a steady state condition. The test conditions have the velocity range of 0.6~2.4 m/s and the tested bubble size is about 4 mm. The imaging process is performed by using a NAC high-speed video camera of which the speed is 1000 fps. The visualization system has a test section which is made of acryl that has the 10mm X 10mm cross-section and a 1 m height. The probe is fixed at the center of the upper side of the test section. The probe that is used in the benchmarking is the 'I' type as shown in figure 6(b). Figure 1 shows the 'L' type to be inserted from the side for practical use. Both probe types have the same features with regards to the sensing part.

Since the flowing bubble has an irregular shape, the exact surface function can be hard to derive mathematically from the photograph. The piercing point is even ambiguous. Therefore, some assumptions in analyzing the bubble samples are adopted.

The flowing bubbles are assumed to be ellipsoidal of which the cross-section perpendicular to the flow direction is a circle. The representative surface function for the bubble can be expressed as follows:

$$\left(\frac{x}{R}\right)^2+\left(\frac{y}{R}\right)^2+\left(\frac{z}{H/2}\right)^2=1 \quad (9)$$

For the upward flowing bubble, the void fraction and interfacial area concentration can then be derived by

$$a=N_b\overline{\left(\frac{h}{V_b}\right)} \approx N_b\overline{\left(\frac{1}{V_b}\right)\left(\frac{H_i}{R_i}\sqrt{R_i^2-\left(x_i^2+y_i^2\right)}\right)_i} \quad (10)$$

and

$$\overline{a_i}=2N_b\overline{\left(\frac{1}{V_b}\sqrt{1+\left(\frac{dz}{dx}\right)_i^2+\left(\frac{dz}{dy}\right)_i^2}\right)} \approx 2N_b\overline{\left(\frac{1}{V_b}\right)}\overline{\sqrt{1+\left(\frac{H}{2R}\right)_i^2\left(\frac{x_i^2+y_i^2}{R_i^2-\left(x_i^2+y_i^2\right)}\right)}} \quad (11)$$

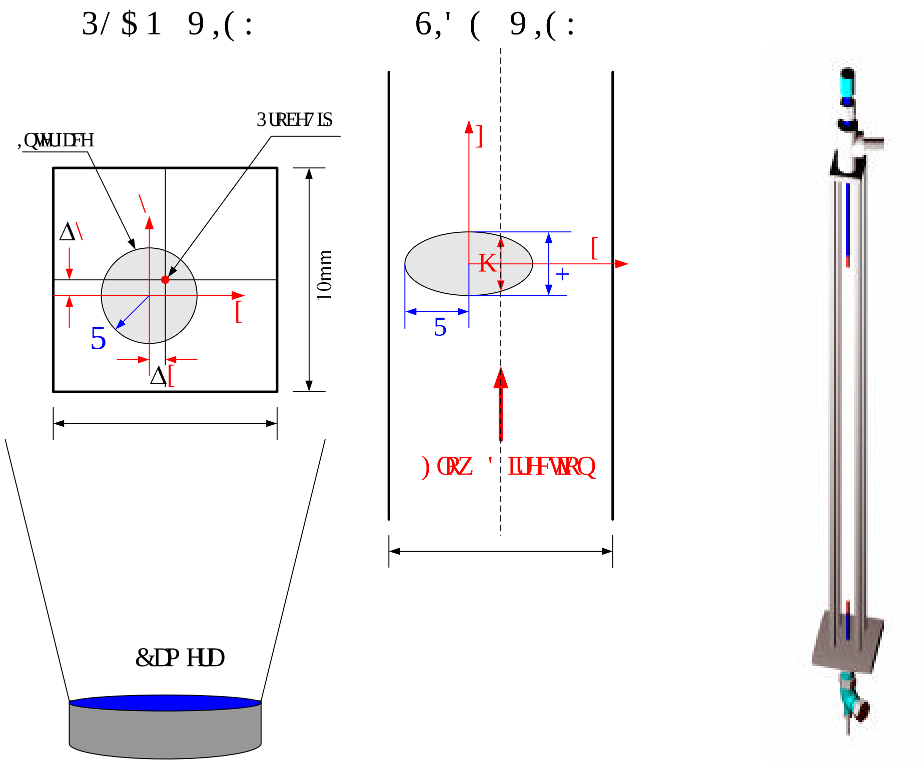

(a) (b)

Figure 6. Imaging System

The Sauter mean diameter can be obtained by Eq.(4).

To apply the above equations, one should know the exact piecing point on the surface. However, it is difficult to measure the explicit point where the sensor tip penetrates the bubble from the photograph. Therefore, we obtained various distributions for the bubble parameters from the bubble samples of the photographs and utilized them for the analysis. The distributions acquired from the bubble samples are for the bubble width, bubble aspect ratio and the position of the bubble center. The parameters can be rewritten by $2R_i$, $(H/2R)_i$, and $(\triangle X/R)_i$ respectively based on figure 6. The distribution of the sensor tip position from the bubble center in the direction of y is assumed to be the same as that in the direction of x since the flow approximates a symmetry condition. The detected bubble frequency, N_b is obtained from the probe data. At least 100 bubble samples that pass the sensor tips in the photograph were utilized for the distributions. Figure 7 shows the typical distribution for the bubble width, 2R, bubble aspect ratio, H/2R, and the distance between the bubble center and the front sensor tip on the x-axis, $\triangle X/R$. For the best fit, “Extreme” and “Gauss” distribution functions were used for the bubble width and aspect ratio, respectively, for this condition. For the piercing point, the interpolation curve is directly used for the distribution. The adopted fitting function can be varied for the best fit.

The various bubble parameters to be used for the image analysis using Eqs. (10) and (11) are then obtained by using the Monte-Carlo method based on the derived distributions. The number of sampled data sets from the distributions is 10000 for every test condition.

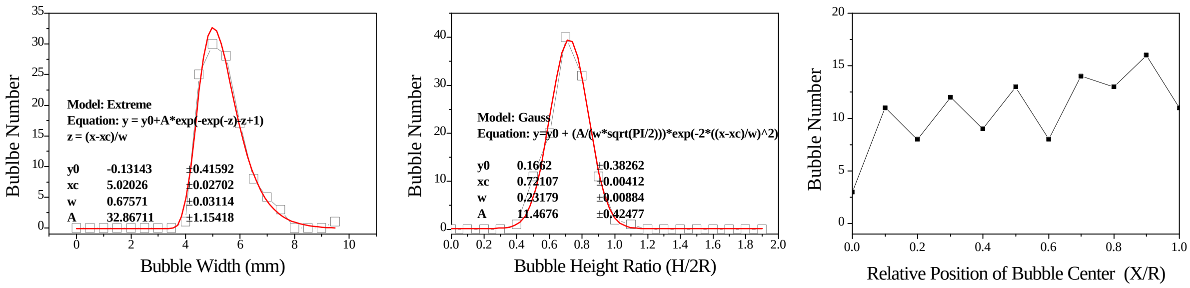

(a) (b) (c)

Figure 7. Typical Distribution of the Bubble Width, Height and Distance between the Bubble Center and the Sensor Tip on the X-axis

6. Results

Since the probe is inserted to the two-phase mixture and directly contacts with the bubble interface, it is important to investigate the deformation of the surface by the sensor tip prior to the study. To reduce the surface perturbation effect, the sensor should be sharply manufactured. Figures 8(a) ~ (c) are the pictures before and after piercing. As shown in the photographs, the bubble has a very little perturbation effect for the motion and geometry of the surface.

(a) (b) (c)

Figure 8. Bubble Penetration through Sensors

The comparison results between the probe and the photographic methods for the various bubble parameters are summarized in table 1. As the results, the velocity agrees well with the 3.7% of the average deviation. The void fraction has a 7.8% deviation. Benchmarking for bubble velocity and void fraction illustrates the interface perturbation effect by the piercing of the sensor tips and the validity of the converting procedures of the raw signals to a rectangular form. Making the raw signals a rectangular form means an explicit definition of the phase for the continuous signals and it is a base for the processing for the various bubble parameters. The small deviations for the two parameters demonstrate the validity of the processing scheme of the probe signals. The average deviations between the two methods for the interfacial area concentration and the Sauter mean diameter are 9.2% and 11.2%, respectively. The error levels are larger than those of the velocity and the void fraction. The parameters are affected by the interface shape. Although the shape of all the bubbles was assumed to be smooth ellipsoidal in this study, the real interface shape is somewhat different from the ideal shape. However, the deviation level between the probe data and the photographic results can be considered to be acceptable. Figures 9(a)~(d) show the plot of the comparison of the velocity, void fraction, IAC and D_{sm}, respectively.

Table 1. Comparison for the Various Bubble Parameters

Case ID	j_f	j_g	Velocity (m/s)			Void Fraction			IAC (1/m)			Dsm (mm)		
	(m/s)	(m/s)	Probe	Photo	Dev. (%)	Probe	Photo	Dev. (%)	Probe	Photo	Dev. (%)	Probe	Photo	Dev. (%)
1	0.30	0.005	0.61	0.63	-3.54	0.022	0.023	-2.64	36.46	32.81	11.12	3.64	4.15	-12.39
2	0.47	0.023	0.91	0.92	-1.33	0.019	0.021	-11.30	32.07	29.75	7.80	3.48	4.23	-17.72
3	0.75	0.049	1.30	1.22	6.23	0.015	0.017	-13.64	24.78	25.28	-1.98	3.63	4.12	-11.90
4	1.00	0.044	1.57	1.45	8.64	0.014	0.016	-8.86	20.17	24.12	-16.38	4.28	3.93	8.99
5	1.50	0.05	2.10	2.13	-1.31	0.037	0.040	-7.00	47.65	49.59	-3.91	4.68	4.84	-3.21
6	1.67	0.088	2.37	2.34	1.32	0.021	0.021	-3.29	30.21	35.15	-14.05	4.09	3.64	12.53

7. Conclusion

A five-sensor conductivity probe method is used to measure the interfacial area concentration in this study. In this study, the design of the probe, signal processing scheme of the raw signals from the probe and the various processes to obtain the physical parameters were described.

To verify the probe method, benchmarking studies were performed by using the photographic method. The comparisons of the two measuring methods are for the velocity, void fraction, interfacial area concentration, and the Sauter mean diameter. Since the interface shape and motion can be hard to measure explicitly at the sensor location from the photograph, statistical approaches were adopted in analyzing the photograph. The soundness of the signal converting process to a rectangular form of the probe signal could be investigated with the comparison of the velocity and void fraction between the two measuring methods. As the results, the velocity and void fraction measured by the probe agree well with those from the photography. The perturbation effect of the probe sensor on the piercing point is found to be trivial from the investigation of the video films and the relevant pictures are presented in the paper.

The IAC and the Sauter mean diameter measured by the five-sensor probe method shows a larger deviation from the photographic data than the velocity and the void fraction. One of the main reasons for the deviation can be considered to be from the assumptions in analyzing the photograph to obtain the interface parameters. Although the flow condition for the visualization is simple, the geometry of the interface is still complex. However, the disagreement can be judged to be within an acceptable range concerning the complexity of the geometry of the bubbles.

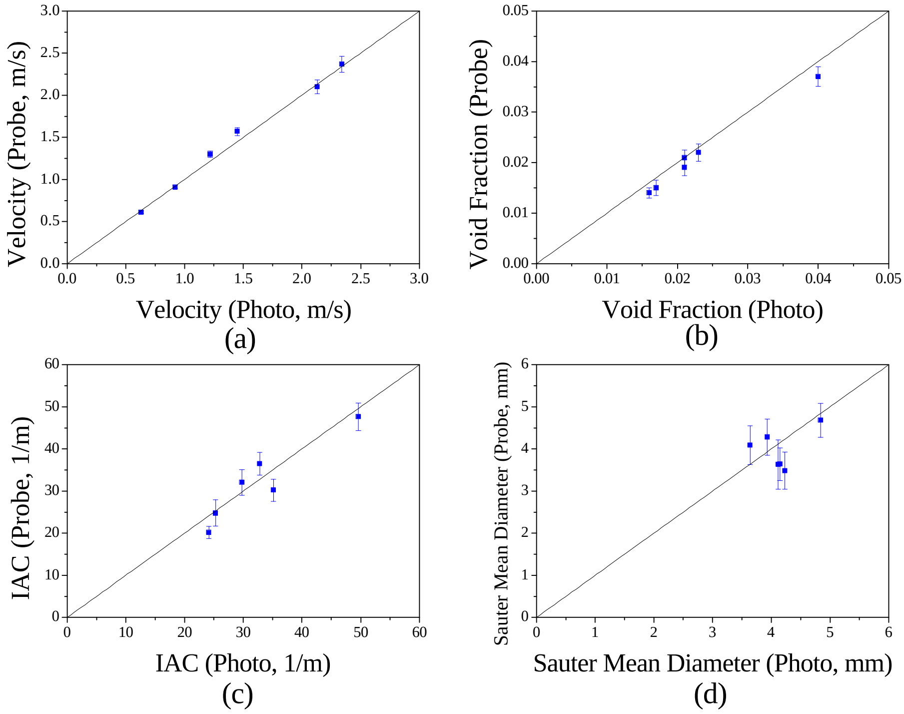

Figure 9. Comparison of the Bubble Parameters

Acknowledgement

This work has been financially supported by the Ministry of Science and Technology (MOST) of Korean government under the national nuclear mid- & long-term R&D program.

References

1. M. Ishii, *Thermo-Fluid Dynamic Theory of Two-Phase Flow*, Eyrolles, Paris, Scientific and Medical Publication of France, New York, 1975
2. I. Kataoka, M. Ishii, A. Serizawa, Local Formulation of Interfacial Area Concentration, *Int. J. Multiphase Flow*, Vol. 12, pp. 505-529, 1986
3. I. Kataoka, A. Serizawa, Interfacial Area Concentration in Bubbly Flow", *Nucl. Eng. Des.*, 120, pp. 163-180, 1990
4. S.T. Revankar, M. Ishii, Local Interfacial Area Measurement in Bubbly Flow, *Int. J. Heat Mass Transfer*, 35(4), pp. 913-925, 1992
5. M.J. Tan, M. Ishii, Interfacial Area Measurement Methods, ANL-89/5, Feb 1989.
6. M. Ishii, S.T. Revankar, Measurement of Interfacial Area Using Four Sensor Probe in Two Phase Flow, DOE/ER/14147, 1991
7. S.T. Revankar, M. Ishii, Theory and Measurement of Local Interfacial Area Using a Four Sensor Probe in Two-Phase Flow, *Int. J. Heat Mass Transfer*, 36, 12, pp. 2997-3007, 1993

8. D.J. Euh, B.J. Yun, C.H. Song, T.S. Kwon, M.K., Chung, U.C. Lee, Development of the Five-Sensor Conductivity Probe Method for the Measurement of the Interfacial Area Condensation, *Nucl. Eng. Des.*, 205, pp.35-51, 2001
9. D.J. Euh, B.J. Yun, C.H. Song, Numerical Simulation for the Improved Five-Sensor Probe Method by Introducing Correction Factors to Measure the Interfacial Area Concentration, *KNS Spring Meeting*, 2004